Extending Galactic foreground models for CMB experiments with GANs

Nicoletta Krachmalnicoff
SISSA, Via Bonomea 265, 34136 Trieste, Italy
INFN, Via Valerio 2, 34127 Trieste, Italy
IFPU, Via Beirut 2, 34014 Trieste, Italy
nkrach@sissa.it

Giuseppe Puglisi
Space Sciences Laboratory, University of California, Berkeley, CA 94720, USA
Computational Cosmology Center, LBNL, Berkeley, CA 94720, USA
gpuglisi@berkeley.edu

Abstract

We present ForSE (Foreground Scale Extender), a novel package which aims at overcoming the current limitations in the simulation of diffuse Galactic radiation, in the context of Cosmic Microwave Background experiments (CMB). ForSE exploits the ability of generative adversarial neural networks (GANs) to learn and reproduce complex features present in a set of images, with the goal of simulating realistic and non-Gaussian foreground radiations at sub-degree angular scales. This is of crucial important in order to be able to estimate the foreground contamination, especially to lensing reconstruction and de-lensing. We have applied our algorithm to Galactic thermal dust emission in both total intensity and polarization. Our results show how ForSE is able to generate small scale features (at 12 arc-minutes) having as input the large scale ones (80 arc-minutes). The injected structures have statistical properties in excellent agreement with the ones of the real sky and show the correct amplitude scaling as a function of the angular dimension.

1 Introduction

The Cosmic Microwave Background (CMB) radiation represents one of the greatest source of knowledge about the history of our Universe. Current and future CMB experiments are focusing on the measurements of its polarized signal, having as main targets (i) the detection of primordial gravitational waves directly linked to the inflation potential and (ii) the precise reconstruction of the gravitational field from the large scale structures that distorts the CMB polarization pattern at the arc-minute scales [1-3]. The achievement of these two ambitious goals will give an unprecedented insight into the evolution of the Universe. As it has appeared evident in the last years, the main limiting factor in such measurements is the contamination coming from Galactic and extra-Galactic radiation, which can be orders of magnitude larger than the target cosmological signal [4]. For this reason having reliable models of foreground emissions, that include the appropriate statistical complexity at all the relevant angular scales (from tens of degrees to few arc-minutes) is crucial, in order to design, test and optimize both the experimental hardware and the data analysis pipelines of future CMB experiments.

In this context, we present a new approach, based on the use of generative adversarial networks (GANs), that aims at overcoming the current limitations in Galactic foreground simulations. As a matter of fact, current models are largely based on available Galactic observations which are either

Third Workshop on Machine Learning and the Physical Sciences (NeurIPS 2020), Vancouver, Canada.

restricted to relatively small sky regions or cover the full Celestial sphere but with poor angular resolution [5]. Our package, named FORSE (Foreground Scale Extender), allows to simulate realistic small scale (sub-degree) features from the real large scale ones.

2 Method

The problem that we want to address can be summarized as follows. Suppose we observe a foreground emission at a given angular resolution and obtain a map M. This can be thought as the combination of a map where only large scale structures are present and a second one with small scale features: $M = M_{LS} + M_{SS}$. We can also make the assumption that the small scale features are modulated by the large ones, with $M_{SS} = M_{LS} \cdot m_{ss}$. In this way we have:

$$\widetilde{m}_{ss} \equiv m_{ss} + 1 = \frac{M}{M_{LS}}. \quad (1)$$

The goal of this work is to use GANs to generate a map of realistic small scale structures ($\widetilde{m}_{ss}$) given the real large scale ones.

The GAN architecture The FORSE package is based on a modified version of the Deep-Convolutional GAN (DCGAN) described in [6], with the main difference being that both the input and the output of the *Generator* (G) are images.

In our architecture G takes as input images of 320×320 pixels which are maps (patches) of the foreground sky where only the large scale features are present (M_{LS}). A series of three convolutional layers is applied, with the dimension of the kernel being 5×5. In the first layer 64 filters are used, and no stride is applied. In the following convolutional layers a stride of 2 is used and the number of filters is doubled. After each convolution, a *LeakyRelu* activation function is applied with slope equal to 0.2, and a *BatchNormalization* layer is added. The decoding part of G is symmetric to the encoding one; upsampling layers are combined with convolutional ones in order to restore the output dimension of the image with 320×320 pixels. The output layer is activated with a *tanh* function.

The *Discriminator* (D), takes as input $\widetilde{m}_{ss}$ images of 320×320 pixels. After three convolutional layers (which are analogous to the encoding part of G) the resulting cube is flattened into a 1-D vector which is then densely connected to the output unit, activated though a *sigmoid* function.

In all our applications, we adopted a *binary cross-entropy* loss function to train our GAN, back-propagating via stochastic gradient descent with mini-batches of $N_b = 16$ images. As suggested in [6], we used the *Adam* optimizer, with a learning rate of 0.0002 and a momentum term $\beta_1 = 0.5$. As a pre-step, all the M_{LS} and the $\widetilde{m}_{ss}^{real}$ patches were normalized, in order to have pixel values in the range $[-1, 1]$.

Note that the GAN architecture that we built is deterministic, with generated small scale structures that only depend on the input large scale ones.

3 Results

We applied our approach to both total intensity and polarization thermal dust maps, as this emission represents one of the main contaminant to CMB observations. In all the considered cases the input of G are maps at 80 arc-minutes angular resolution while the output is at $12'$. We used the dust template obtained from the GNILC (Generalized Needlet Internal Linear Combination) method at 353 GHz. The GNILC dust maps have an angular resolution that varies in the sky and depends on the signal-to-noise ratio (SNR) of the Planck high frequency maps: in total intensity the effective beam FWHM (full width half maximum) ranges from 5 to about 22 arc-minutes, while in polarization it varies in the interval $5 - 80$ arc-minutes [7] .

Total Intensity We firstly tested the ability of FORSE of generating realistic small scale features in total intensity (quantified by the Stokes I parameter). In order to train the GAN, a set of patches for which both the large scale (M_{LS}) and the small structures ($\widetilde{m}_{ss}^{real}$) are known is needed . As stated above, the GNILC template in total intensity has a variable angular resolution, which is equal to 5 arc-minutes in the regions close to the Galactic plane, making them suitable to be used to perform

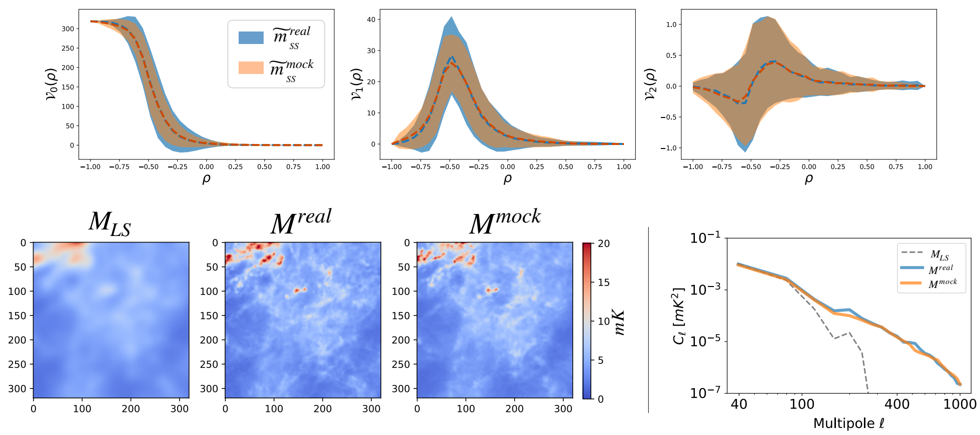

Figure 1: Upper panels: Minkowski functionals as a function of the threshold ρ, for $\widetilde{m}_{SS}^{real}$ (blue) $\widetilde{m}_{SS}^{mock}$ (orange), for the case of total intensity dust maps. The functionals are computed for the 350 patches used to train the GAN and we report the mean (dashed lines) and 1σ deviation (shaded areas) of the distributions. The high level of superposition between the curves demonstrates the ability of ForSE to reproduce the correct statistical properties of small scale foregrounds. Lower panel: M_{LS} and M^{real} represent the real low resolution ($80'$) and high resolution ($12'$) images of a patch in the sky, respectively. In M^{mock} the small scale structures ($< 80'$) have been generated by ForSE. On the right the related angular power spectra are shown. Notice that the fact the spectrum of M_{LS} drops at $\ell \sim 300$ is an effect due to the lower resolution in the map lacking of small scale power.

training.Ṫhe M_{LS} patches were thus generated as tiles of $20^\circ \times 20^\circ$ and 320×320 pixels from the GNILC I template smoothed at the angular resolution of 80 arc-minutes. On the other hand, $\widetilde{m}_{SS}^{real}$ patches were obtained from the same GNILC map smoothed at 12 arc-minutes angular resolution and divided by M_{LS} (see definition in Eq. 1). All the tiles were taken from the region of the sky where the GNLIC template has the finest angular resolution and it is less contaminated by noise, for a total of 350 pair of images.

In the upper panels of Figure 1, we show a comparison of the generated small scale structures with the real ones, from a statistical point of view. We used the Minkowski functionals, as defined in [8], which are sensitive to the presence of non-Gaussian structures and are more effectively able to distinguish them from Gaussian ones with respect to other methods, e.g. Peak signal to Noise ratio or Multi Scale Structural Similarity index. The distribution of the functionals for the two sets of images presents a remarkable agreement, with superposition at the level of 76% ($\mathcal{V}_0$), 84% ($\mathcal{V}_1$) and 91% ($\mathcal{V}_2$). This results clearly show how the approach developed with ForSE allows to generate small scale feature on foreground maps that match the statistical properties of the real ones.

Once the small scale features are generated by the GAN they need to be normalized back in order to restore physical units. In this case, where we tested the feasibility of the approach in total intensity, the normalization to physical units is trivial, as, for each considered patch, we know the amplitude of the real small scales structures and we can therefore use this information. Once physical units are restored, we combined the large and small scale patches and got the final images as $M = M_{LS} \cdot \widetilde{m}_{SS}$ (see relation 1), shown in the lower panels of Figure 1. The comparison of the combined M^{mock} and M^{real} images and the corresponding power spectra not only shows that ForSE generates small scale structures with realistic morphology and statistical properties, but also that the correct amplitude scaling as a function of the angular scale is recovered.

Polarization The GNILC polarized thermal dust template has an angular resolution below 12 arc-minutes (the target resolution of ForSE) only in about 9% of the sky and mainly in the inner Galactic plane region ($|b| < 10^\circ$). Given this lack of high resolution data, we could not apply the procedure used in total intensity and train the GAN directly in polarization. To overcome this limitation, we made the assumption that small scale structures in polarization follow the same statistics as the ones in total intensity. This represents a reasonable assumption to the first order; in fact, we can assume

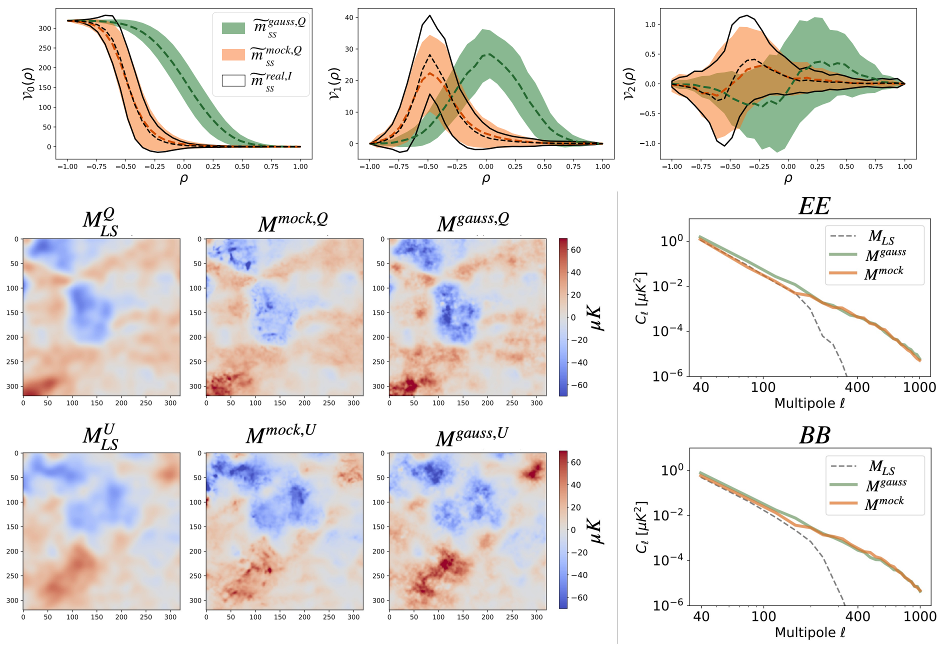

Figure 2: Upper panels: Minkowski functionals for real small scale structures in total intensity (black lines), features generated by the GAN on Q maps (orange) and Gaussian ones (green). Lower panel, from left to right: input low resolution Q and U maps, results obtained from our GAN approach, maps with Gaussian small scale features. On the right the corresponding polarization power spectra are shown.

that the dust grains population producing the polarized emission is the same as the one responsible in emitting the unpolarized signal. Additionally, we know that thermal dust radiation has similar two point correlation functions (power spectra) in polarization and total intensity [9].

With this assumption, we proceeded by training separately two different GANs, for Stokes Q and U patches respectively. In particular, we use as input to G, low resolution images $M_{LS}^{Q(U)}$ taken from the GNILC Stokes Q (U) maps. The generated outputs are compared by D with the real small scale structures in total intensity ($\widetilde{m}_{SS}^{real,I}$) and the GAN weights are thus optimized in order to make $\widetilde{m}_{SS}^{mock,Q(U)}$ indistinguishable from $\widetilde{m}_{SS}^{real,I}$.

In the upper panels of Figure 2 we report the Minkowski functionals for the Stokes Q case. The distributions of the mock structures are in good agreement with the real total intensity ones, with a superposition of ($\mathcal{V}_0$, $\mathcal{V}_1$, $\mathcal{V}_2$) at the level of $(85\%, 80\%, 86\%)$ respectively (similar for U maps). We also compare the statistics of the generated maps with the one of small scale features obtained as simple Gaussian realizations of the extrapolation of the dust power spectra ($\widetilde{m}_{SS}^{gauss,Q(U)}$). Results show how the GAN is able to generate highly non-Gaussian structures. In the lower panels of Figure 2, we present the final polarization Q and U maps and their power spectra, after the combination of the real large scales structures and the small ones generated by the GAN. The latter have been re-normalized to physical units by matching their amplitude with the one of the Gaussian $\widetilde{m}_{SS}^{gauss,Q(U)}$ maps, leading to the correct scaling as a function of multipoles.

The full sky polarization Stokes Q and U maps obtained with our approach are publicly available for download at `https://portal.nersc.gov/project/sobs/users/ForSE/`.

4 Discussion and Conclusions

In this work we have presented a novel approach, based on the use of GANs, to simulate realistic non-Gaussian sub-degree Galactic foreground emission in the context of CMB observations. We have applied our algorithm, named ForSE, to thermal dust radiation considering both total intensity and polarized signal. In all the cases, we have trained the GAN to generate small scale structures, at 12 arc-minutes, starting from low resolution images, at 80 arc-minutes. Our results demonstrate how FORSE is able to generate small scale features with statistical properties that match the real ones and are highly non-Gaussian. Moreover the amplitude of the simulated structures follow the correct scaling as a function of the angular scale.

The approach presented in this work could be further developed. In particular, it could be used to further extend the angular resolution of foreground models at even smaller scales. This could be done by making use of new high resolution data that will become publicly available in the coming years (for example ACTpol [2]). The second way would be to train and apply the GAN predictions iteratively, in a sort of "fractal" approach, by considering the foreground statistical properties as scale invariant. Lastly, one could think about training the neural network to learn and reproduce the relation between large and small structures as well as their statical properties on numerical magnetohydrodynamic (MHD) simulations, and then apply it to real low resolution data. Of course, although we have applied FORSE only to thermal dust emission, nothing prevents us to use it on other kind of emissions, as long as a sufficient amount of data exists.

Impact statement

Our work relies on the use of GANs with the goal of enhancing and complementing available models of the diffuse Galactic emission. We have applied the method in the context of CMB science, where foreground emission represents a strong limiting factor. In particular, the lack of full sky high resolution Galactic data in polarization represents a challenge, as such information is needed in order to prepare and optimize the next generation of CMB experiments. The use of artificial intelligence techniques allows to fill this gap, until new and precise data will come. Of course, our approach could be applied in other fields in Astrophysics and Cosmology; namely whenever simulations of a given astrophysical component are needed and sufficient information are available to train the network. The codes that we developed will be made available in a python package, named FORSE, that we are currently wrapping up for publication. The word "forse", which means "maybe" in Italian, emphasizes the fact that the small scale structures that the algorithm generates are not supposed to correspond, morphologically, to the real ones, but only to resemble their statistics. It is however true that this approach allows to generate fake data that might be indistinguishable from real ones. Nonetheless the author do not forsee this as an ethical issue, at least for what concerns astrophysical applications. As a matter of fact, in this scientific field, the use of realistic simulations of data is common since decades, and the community certainly possesses the background and awareness necessary to correctly exploit them.

Acknowledgments and Disclosure of Funding

NK acknowledges support from the ASI-Cosmos and ASI-LiteBIRD programs, from the INDARK and LiteBIRD INFN initiatives and from the "Leonardo da Vinci" grant (MIUR-2019). NK also thanks the Simons Foundation for hosting her at the Flatiron Institute (New York, USA) in fall 2019, and the whole group of Cosmology x Data Science at CCA (Center for Computational Astrophysics) for the extremely useful discussions at the beginning of this work. This research used resources of the National Energy Research Scientific Computing Center (NERSC), a U.S. Department of Energy Office of Science User Facility operated under Contract No. DE-AC02-05CH11231.

References

[1] The Simons Observatory Collaboration. 2019, JCAP, 2019, 056

[2] Aiola, S., Calabrese, E., Maurin, L., et al. 2020, arXiv e-prints, arXiv:2007.07288

[3] Sugai, H., Ade, P. A. R., Akiba, Y., et al. 2020, Journal of Low Temperature Physics, 199, 1107

[4] Krachmalnicoff, N., Carretti, E., Baccigalupi, C., et al. 2018, A&A, 618, A166

[5] Thorne, B., Dunkley, J., Alonso, D., & Næss, S. 2017, MNRAS, 469, 2821

[6] Radford, A., Metz, L., & Chintala, S. 2016, in 4th International Conference on Learning Representations, ICLR 2016, San Juan, Puerto Rico, May 2-4, 2016, Conference Track Proceedings, ed. Y. Bengio & Y. LeCun

[7] Planck Collaboration Int. XLVIII. 2016, A&A, 596, A109

[8] Mantz, H., Jacobs, K., & Mecke, K. 2008, J. Stat. Mech. P12015 J. Stat. Mech, 12

[9] Planck Collaboration XI. 2020, A&A, 641, A11